Current Biology 16, 1748–1756, September 5, 2006 ©2006 Elsevier Ltd All rights reserved DOI 10.1016/j.cub.2006.06.067

Report

MEL-28, a Novel Nuclear-Envelope and Kinetochore Protein Essential for Zygotic Nuclear-Envelope Assembly in *C. elegans*

Vincent Galy,[1,2,5] Peter Askjaer,[1,3,5] Cerstin Franz,[1] Carmen López-Iglesias,[4] and Iain W. Mattaj[1,*]

[1] European Molecular Biology Laboratory
Meyerhofstrasse 1
69117 Heidelberg
Germany

[2] Institut Pasteur
Centre National de la Recherche
Scientifique-Interactions et Dynamique Cellulaires
25 rue du Docteur Roux
75724 Paris cedex 15
France

[3] Institute for Research in Biomedicine
Barcelona Science Park IRB-PCB
Josep Samitier 1-5
08028 Barcelona
Spain

[4] University of Barcelona
Barcelona Science Park SCT-UB
Josep Samitier 1-5
08028 Barcelona
Spain

Summary

The nuclear envelope (NE) of eukaryotic cells separates nucleoplasm from cytoplasm, mediates nucleocytoplasmic transport, and contributes to the control of gene expression [1, 2]. The NE consists of three major components: the nuclear membranes, the nuclear pore complexes (NPCs), and the nuclear lamina. The list of identified NE proteins has increased considerably during recent years but is most likely not complete. In most eukaryotes, the NE breaks down and is then reassembled during mitosis. The assembly of NPCs and the association and fusion of nuclear membranes around decondensing chromosomes are tightly coordinated processes [3]. Here, we report the identification and characterization of MEL-28, a large protein essential for the assembly of a functional NE in *C. elegans* embryos. RNAi depletion or genetic mutation of *mel-28* severely impairs nuclear morphology and leads to abnormal distribution of both integral NE proteins and NPCs. The structural defects of the NE were associated with functional defects and lack of nuclear exclusion of soluble proteins. MEL-28 localizes to NPCs during interphase, to kinetochores in early to middle mitosis then is widely distributed on chromatin late in mitosis. We show that MEL-28 is an early-assembling, stable NE component required for all aspects of NE assembly.

*Correspondence: mattaj@embl.de

[5] These authors contributed equally to this work.

Results and Discussion

Identification of MEL-28, a Conserved Protein Required for Normal Nuclear Morphology

To identify novel proteins required for nuclear-envelope (NE) reformation after mitosis in early *C. elegans* embryos, we analyzed genes that were found to influence nuclear morphology in large-scale RNAi screens [4–6]. Of the seven uncharacterized candidates targeted, C38D4.3 was particularly interesting because of the strong and reproducible nuclear defects visible by differential interference contrast microscopy (see below). This phenotype was similar to the phenotype described previously for the maternal-effect embryonic-lethal mutation *mel-28*, which maps to a 1.66 Mb deficiency (sDf121 [7]) including C38D4.3 among 281 other predicted or known genes on chromosome III. We PCR amplified and sequenced the C38D4.3 gene from *mel-28(t1684)* and *mel-28(t1578)* mutants and found base substitutions that introduce a premature termination codon in each case (see Figure S1A in the Supplemental Data available online). Immunofluorescence microscopy with antibodies against amino acids 990–1237 of C38D4.3 detected no gene product in *mel-28(t1684*, *t1587*, *t1579*, or *t1589)* embryos (data not shown). Finally, expression of affinity-tagged C38D4.3 restored the hatching rate of *mel-28(t1579)* embryos from 0% to 42%, confirming the mutation in C38D4.3 as the sole cause of the *mel-28* mutant phenotype (data not shown). We will refer to C38D4.3 as *mel-28*.

mel-28 encodes a large protein that has a predicted molecular weight of 201 kDa and that does not possess extensive sequence similarity to known proteins. Domain analysis revealed the presence of a very short central domain with a high probability to form a coiled-coil structure and one or possibly two C-terminal putative AT-rich DNA binding domains (AT-hook domains, Figure S1A). Sequence-homology searches led to the identification of potential orthologs in another nematode (*C. briggsae*) and in vertebrates (*H. sapiens* and *X. laevis*) (Figure S1B). The sequence conservation outside the nematode phylum was low, and we analyzed the genes identified both in *C. briggsae* and in *X. laevis*. The *C. briggsae* genome contains two genes that are both similar to *C. elegans mel-28*. Injection of dsRNA designed to target both genes resulted in a nuclear-appearance-defect phenotype strikingly similar to that observed in *C. elegans mel-28(t1684)* embryos (Figure S2; compare with Figure 1). Moreover, the protein we identified in *Xenopus* shows similar subcellular localization to *C. elegans* MEL-28 (our unpublished data). We thus conclude that MEL-28 is a conserved protein.

mel-28(t1684) is recessive, and homozygous *mel-28(t1684)* hermaphrodites develop into adults producing only dead embryos [7], which we refer to as *mel-28(t1684)* embryos. The strong nuclear-morphological defects previously observed by time-lapse DIC microscopy analysis [7] were fully penetrant (data not shown;

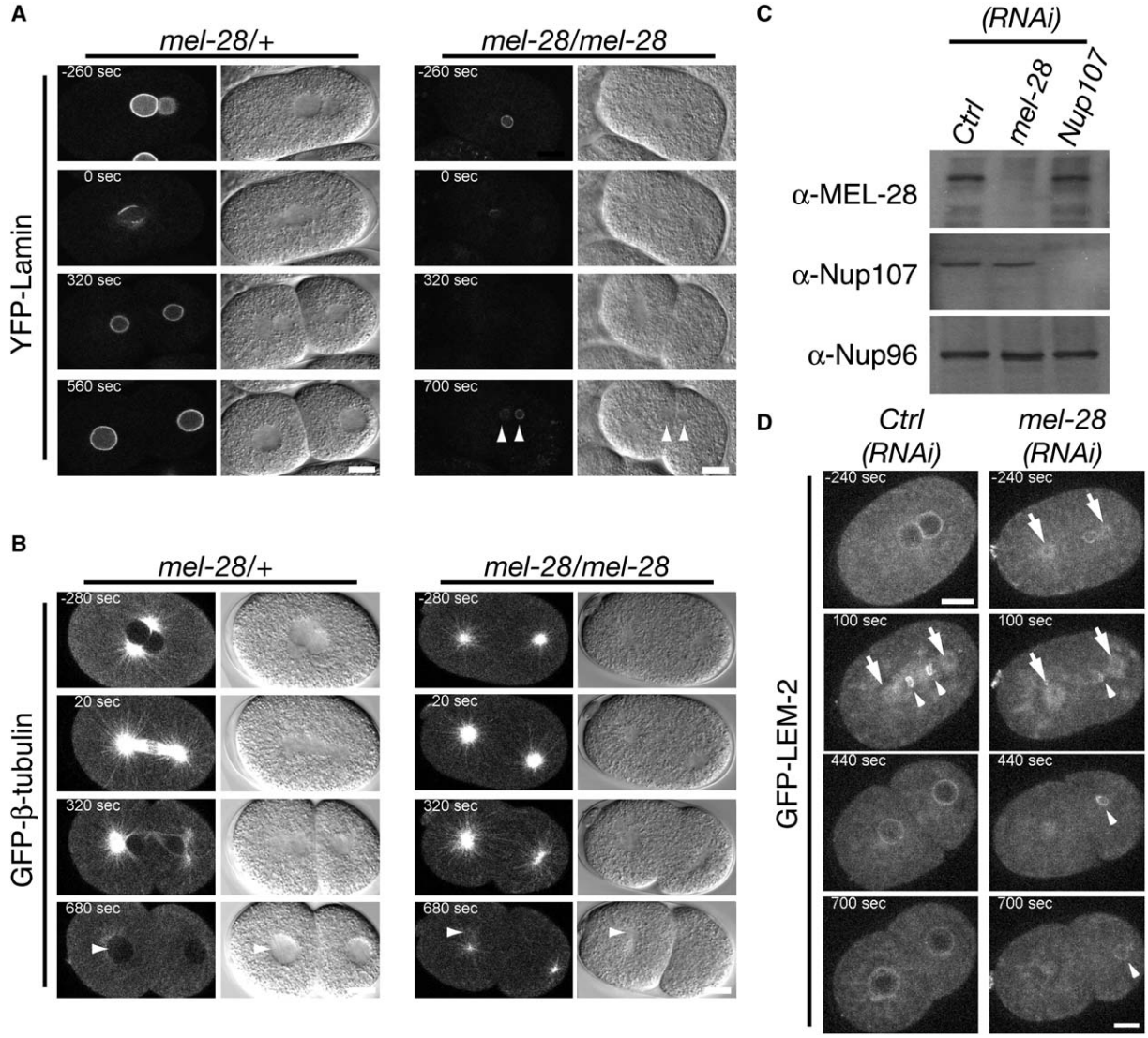

Figure 1. Inhibition of *mel-28* Leads to Structural and Functional NE Defects

(A) Still images of YFP-Lamin (left) and DIC (right) from confocal time-lapse microscopy recordings of embryos from heterozygous (left column) or homozygous (right column) *mel-28(t1684)* nematodes expressing YFP-Lamin. Note a strong reduction of YFP-Lamin nuclear accumulation in mutant embryos (arrowheads).

(B) Still images of GFP (left) and DIC (right) from confocal time-lapse microscopy recordings of embryos from heterozygous (left column) or homozygous (right column) *mel-28(t1684)* nematodes expressing GFP-β-tubulin. There is a lack of exclusion of soluble GFP-β-tubulin from the nuclear space in the mutant embryo (compare arrowheads).

(C) Total protein extracts from control RNAi (left lane), *mel-28(RNAi)* (middle lane), or *Nup107(RNAi)* (right lane) embryos were analyzed by Western blotting with polyclonal antibodies against MEL-28 (upper panel), Nup107 (middle panel), or Nup96 (lower panel). *mel-28(RNAi)* efficiently and specifically depleted MEL-28 protein.

(D) Z-projection from 4D confocal time-lapse microscopy recordings of GFP-LEM-2 expressing embryos from worms treated with control (left) or *mel-28* (right) RNAi-feeding bacteria. GFP-LEM-2 accumulated around centrosomes (arrows) in *mel-28(RNAi)* embryos, whereas pronuclei were hardly visible (t = −240 s). GFP-LEM-2 in *mel-28(RNAi)* embryos reassociated poorly with chromatin (arrowheads) after mitosis, and nuclear growth was not observed (440–700 s). Scale bars represent 10 μm. Time is indicated relative to first anaphase onset.

see Figures 1A and 1B). These results suggest that maternal MEL-28 is essential in the embryo and that either MEL-28 is dispensable for larval development or maternal MEL-28 is sufficient to allow development to adulthood. However, we cannot rule out that *mel-28(t1684)* might be a hypomorphic allele that supports larval but not embryonic development. Because RNAi treatment with dsRNA corresponding to *mel-28* specifically reduced the amount of MEL-28 in embryo extract to less than 5% (Figure 1C), affected mitotic progression of all the young embryos observed, and caused 100% (±0, n = 1325) embryonic lethality, we conclude that maternal MEL-28 is essential for embryo development.

MEL-28 Is Required for NE Formation and Function

Pronuclear- and nuclear- morphology defects observed with DIC microscopy can be caused by defects in various processes, including chromatin segregation,

nucleo-cytoplasmic transport, and NE reformation. In order to discriminate between these different options, we characterized the effects of the *mel-28(t1684)* allele and MEL-28 depletion by RNAi on NE structure and function.

We crossed *mel-28(t1684)* with a strain expressing yellow fluorescent protein fused to *C. elegans* lamin (YFP-LMN-1 [8]) and monitored its distribution in early embryos. Whereas YFP-LMN-1 displayed strong NE staining in embryos from heterozygous worms, in *mel-28(t1684)* embryos, very little YFP-LMN-1 was present around the chromatin of pronuclei or in interphase after the first mitotic division (Figure 1A).

The defect in nuclear lamin localization prompted us to test the functionality of the NE in *mel-28* mutants. A functional NE forms a physical barrier excluding large soluble cytoplasmic proteins such as GFP-β-tubulin. Wild-type embryos (data not shown) and embryos from heterozygotes excluded soluble GFP-β-tubulin from pronuclei of one-cell embryos (Figure 1B, −280 s on the left; see also Movie S1) as well as from nuclei of two-cell embryos (Figure 1B, 680 s on the left). In *mel-28(t1684)* embryos, neither pronuclear nor nuclear exclusion was detected (Figure 1B, −280 s and 680 s on the right), revealing a lack of a functional NE around chromatin. Taken together, these results suggested that *mel-28(t1684)* mutation affects the formation or the maintenance of a functional NE rather than nucleo-cytoplasmic transport. This conclusion is supported by the observation that RNAi depletion of several nucleoporins involved in nucleo-cytoplasmic transport affects nuclear growth and size without preventing nuclear formation [8].

Next, we tested the effect of MEL-28 depletion on the distribution of the integral NE protein GFP-LEM-2 [8–10]. After control RNAi treatment, GFP-LEM-2 was evenly distributed in pronuclear NEs, redistributed to the endoplasmic reticulum (ER) during mitosis, and recruited around chromosomes 60–100 s after anaphase entry (Figure 1D, left column). In *mel-28(RNAi)* one-cell embryos, no clear nuclear rim staining was visible despite the acquisition of several confocal sections at each time point. Small and misshapen pronuclei were sometime seen, and GFP signal concentrated around the centrosomes prior to mitosis. Later during mitosis, more GFP-LEM-2 accumulated at centrosomes than in control RNAi-treated embryos, but mitosis proceeded normally in terms of centrosome "rocking" and cytokinesis. At mitotic exit, GFP-LEM-2 signal on the chromatin surface increased to a lesser degree than in the control RNAi embryos (Figure 1D, 100 s in the right column) and at best formed a discontinuous, small, and misshapen NE-like structure. A very similar phenotype was observed for another inner-nuclear-membrane protein, Emerin (Figure S3).

The NE defect did not reflect a general defect in endomembrane organization because no significant difference in the ER localization of GFP-SP12 ([11]) was observed between control and *mel-28(RNAi)*-treated embryos except in the region of the nuclear envelope (Figure S4).

In order to directly test the effect of MEL-28 depletion on chromatin segregation, we performed RNAi depletion in worms expressing GFP-β-tubulin and GFP-histone H2B. We observed severe defects in the shape and organization of the chromatin masses at the pronuclear stage in *mel-28(RNAi)* embryos, and the physical association of the centrosomes with chromatin was often lost (Figure S5A). Severe chromatin-segregation defects leading to abnormal chromatin distribution were reproducibly observed. A phenocopy of the segregation defect was obtained by RNAi depletion of Ce-CENP-A, a component of the kinetochore encoded by *hcp-3* [12]. Despite the strong segregation defects observed in *hcp-3(RNAi)* embryos, nuclear growth was not affected, and normal nuclear accumulation of lamin as well as nuclear exclusion of GFP-β-tubulin were observed, indicative of a functional NE (Figure S5B). This demonstrates that defects in chromosome segregation do not per se affect NE formation. In conclusion, these data demonstrate that MEL-28 is required for the formation of a functional NE.

MEL-28 Is a Nuclear-Envelope Protein Associated with Kinetochores during Mitosis

In order to better understand how MEL-28 regulates NE assembly, we analyzed its localization and dynamics during cell division. MEL-28 was expressed in embryos as well as in all larval stages and in adults (data not shown). Immunolocalization of MEL-28 in several tissues revealed a nuclear-rim localization typical for NE or NPC proteins (Figure 2A; see also Figure S6). Interestingly, MEL-28 was localized to chromatin during mitosis (Figures 2A and 3A). The immunolocalization of endogenous MEL-28 was similar to the localization of GFP-tagged C38D4.3 (i.e., MEL28) reported by Gunsalus et al. [13]. The localization of MEL-28 within the NE was then analyzed by immuno-gold TEM. As expected, the highest density of gold particles was observed at the NE, but particles were also observed in the nucleoplasm and the cytoplasm (Table S1). Particles found in the cytoplasm most likely reflect a cross reactivity of the MEL-28 antibody because a similar density of gold particles was observed in the cytoplasm of *mel-28(t1684)* embryos. No gold particles were observed in the nuclei or at the nuclear periphery of mutant embryos (data not shown). Importantly, of the particles associated with the NE in the wild-types, 95.0% (152/160) were found at NPCs (Figure 2B; see also Table S1). No accumulation at the outer nuclear membrane was detected. MEL-28 enrichment at NPCs was also detected in gonad nuclei (data not shown). We conclude that MEL-28 is a nuclear-envelope protein enriched at NPCs.

Interestingly, immunofluorescence analysis revealed that MEL-28 began to localize to the condensing chromosomes before complete disappearance of mAb414 staining from the nuclear rim at prophase and began to appear as two lines parallel to the metaphase plate (Figures 2A and 2C). During late anaphase, MEL-28 signal colocalized with the decondensing chromosomes, and the mAb414 signal reaccumulated to the reforming NE during telophase (Figures 2A and 2C). We compared the localization of MEL-28 with that of HIM-10, an outer-kinetochore component [14]. Immunolocalization of MEL-28 in embryos expressing GFP-HIM-10 revealed an overlapping localization of both proteins parallel to the metaphase plate within the mitotic spindle (Figure 2D). This prompted us to test whether the kinetochore localization of MEL-28 required spindle microtubules.

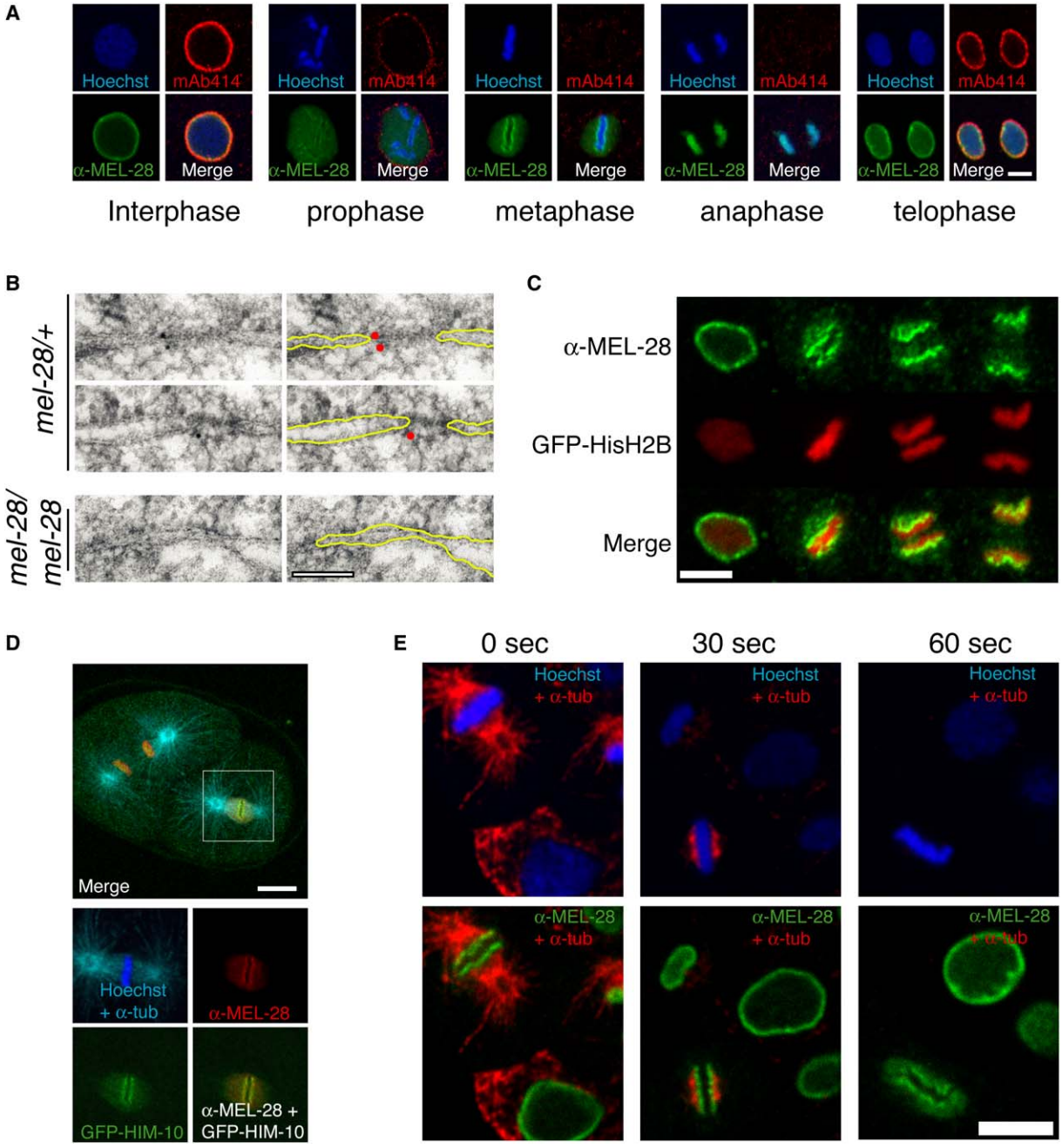

Figure 2. MEL-28 Is an NE Protein during Interphase and Associates with Chromosomes in Mitosis

(A) Immunolocalization of MEL-28 (green), mAb414-reactive nucleoporins (red), and chromatin with Hoechst (blue) showed a dynamic behavior, including NE accumulation (interphase) and kinetochore localization (metaphase) for MEL-28. The scale bar represents 5 μm.

(B) Immuno-gold localization of MEL-28 in embryos from heterozygous (upper two rows) or homozygous (lower row) *mel-28(t1684)* nematodes revealed an enrichment at NPCs. NE membranes (yellow) and gold particles (red) are highlighted (right column). The scale bar represents 100 nm.

(C) Immunolocalization of MEL-28 (green) in embryos expressing GFP-histone H2B (red) indicated that MEL-28 was mostly associated with the chromosome surfaces facing the spindle poles through metaphase and anaphase (three right columns). The scale bar represents 5 μm.

(D) Colocalization of MEL-28 (red) with the kinetochore component GFP-HIM-10 (green). Microtubules are light blue, and DNA is stained with Hoechst (dark blue). The scale bar represents 10 μm.

(E) Immunolocalization of MEL-28 (green), microtubules (red), and chromatin (blue) revealed a stable and microtubule-independent kinetochore localization of MEL-28 during metaphase both before (0 s) and after treatment on ice for 30 or 60 s prior to fixation. The scale bar represents 5 μm.

Only a few kinetochore microtubules remained visible after 30 s on ice, and after 60 s, microtubules were not detectable (Figure 2E). At both time points, MEL-28 staining remained clearly visible along the condensed and aligned chromosomes. From these results, we conclude that MEL-28 localizes to kinetochores during mitosis. The potential kinetochore function of MEL-28 was not addressed further, but the chromosome-segregation defects described above suggest that it may indeed be important in this context. The dual localization

at the NE and kinetochore is reminiscent of several known NE components, including the Nup107-160 NPC sub-complex [15–17] and RanBP2 (Nup358) [15]. Moreover, RanBP2 (Nup358) was shown to be required for chromosome segregation in *C. elegans* embryos and mammalians cells [15, 18]. Interestingly, MEL-28 localization changes rapidly at late anaphase and telophase. MEL-28 initially spreads over the entire chromatin surface then rapidly relocalizes to the NE. This distribution would be consistent with MEL-28's playing a role in the interactions that occur between chromatin and the assembling NE and NPCs late in mitosis.

MEL-28 Is an Early-Assembling and Stable Nuclear-Envelope Protein

To investigate the dynamics of MEL-28 in living embryos, we compared GFP-MEL-28 with known NE proteins fused to G/YFP by using confocal time-lapse microscopy. Like endogenous MEL-28, which was localized by immunostaining, GFP-MEL-28 was mostly concentrated at the nuclear periphery but was also detected in the nucleoplasm and associated with condensing chromosomes when cells entered mitosis (Figure 3A; see also Movie S2). This pattern was indistinguishable from that of YFP-Nup107, which also localizes to kinetochores and is recruited very early during NE assembly (Figure 3A [16, 17, 19]). Consistent with previous reports, GFP-Nup155 associated with the NE approximately 60 s after anaphase onset (Figure 3A) when the integral NE protein LEM-2 began to concentrate around chromosomes (Figure 3A). Thus, MEL-28 is present on chromatin before NE reassembly and earlier than most other NE components, consistent with an important function for MEL-28 during NE assembly.

The observation that MEL-28 localizes at the nuclear periphery and is required for the assembly of a functional NE suggested that MEL-28 could be an architectural component of the NE. In order to test this hypothesis, we estimated the turnover of GFP-MEL-28 at the NE by measuring fluorescence recovery after photobleaching (FRAP). One third of the nuclear volume of fully grown nuclei of four-cell-stage embryos was bleached with high-intensity laser irradiation, and the recovery of fluorescence was monitored (Figure 3B). Only approximately 20% recovery of NE-associated GFP-MEL-28 was observed between the bleaching and the next NE breakdown (Figure 3B, top and bottom). The recovery rate was significantly lower than for GFP-Nup155 ($\sim$60%, Figure 3B) but similar to that of lamin and Nup107 (Figure 3B, bottom), which have both been shown to be very stable NE components in vertebrates [20, 21]. In contrast to the low turnover of GFP-MEL-28 at the NE, the nucleoplasmic pool was highly mobile (Figures 3B and 3C). To analyze this in detail, we compared the dynamics of NE-associated and nucleoplasmic pools of GFP-MEL-28 by measuring fluorescence loss in photobleaching (FLIP). Consistent with the FRAP data, after approximately 23 s, the nucleoplasmic fluorescence intensity was reduced by half, whereas the NE signal was only reduced by approximately 15% (Figure 3C). This suggested a high turnover of the nucleoplasmic pool and a stable association of GFP-MEL-28 at the NE. These results suggest that MEL-28 is a stable as well as an early-assembling component of the *C. elegans* NE.

MEL-28 Inactivation Induces Strong Nuclear-Membrane Defects and Reduces NPC Density

For the evaluation of the ultrastructural NE defects caused by MEL-28 depletion, embryos were processed for transmission electron microscopy (TEM). Nuclei in embryos from *mel-28(t1684)* heterozygous animals were surrounded by continuous NEs containing a similar density of NPCs to wild-type animals (Figure 4A, top; data not shown). In contrast, *mel-28(t1684)* embryos were characterized by abnormal nuclei that were not enclosed by NEs. Much of the chromatin surface was devoid of nuclear membranes, whereas other regions were associated with patches of membrane lacking NPCs (Figure 4A, middle and bottom). DIC microscopy of *mel-28(t1684)* embryos after the four-cell stage suggested that a small number of seemingly normal nuclei might be present (data not shown); however, the TEM analysis demonstrated that these nuclei have several defects including a dramatically reduced density of NPCs and areas of chromatin not covered by nuclear membranes. In conclusion, MEL-28 is required for numerous aspects of NE assembly including NPC formation and enclosure of chromatin by nuclear membranes.

The decreased number of NPCs visible by TEM (Figure 4A), as well as the abnormal mAb414 staining of *mel-28(t1684)* embryos (data not shown), indicated that MEL-28 is required for postmitotic NPC assembly. To analyze in greater detail at which step MEL-28 is required, we investigated the localization of individual NPC components in *mel-28(RNAi)* embryos. Consistent with Western-blot analysis (Figure 1C), RNAi against MEL-28 significantly reduced the amount of MEL-28 protein detected in young embryos and affected the distribution of NPC components recognized by mAb414 (Figure 4B). mAb414 recognizes at least three known *C. elegans* nucleoporins: Nup358, Nup96, and Nup98 [8]. Nup96 is part of the Nup107-160 NPC subcomplex, whose association with chromatin is required early in NPC assembly in vertebrates [19, 22]. We tested whether MEL-28 is needed for the recruitment of Nup96 and Nup107, two components of this complex (Figure 4C). Although both proteins were localized at the nuclear periphery of control RNAi-treated embryos, the chromatin-associated signal was strongly reduced in the absence of MEL-28, suggesting that MEL-28 is required for early steps of NPC assembly. Western-blot analysis showed that MEL-28 RNAi depletion did not affect the total amount of Nup96 and Nup107 (Figure 1C).

In conclusion, the analysis by TEM confirmed both that NE assembly was incomplete in the absence of MEL-28 and that NPC density was dramatically reduced. These data suggest that MEL-28 has a critical role in NE assembly, and its presence on chromatin immediately prior to assembly is suggestive of an early role, perhaps in membrane or nucleoporin association with chromatin. This hypothesis is consistent with an early block of in vitro nuclear-envelope assembly observed upon immunodepletion of *Xenopus* MEL-28 (C.F. et al., unpublished data). The enrichment of gold particles at the NPC in immuno-gold TEM localization of MEL-28 suggests that it is associated with NPCs, although it has not previously been identified as a component of biochemically isolated metazoan NPCs [23]. Our attempts to test for a physical interaction between *C. elegans*

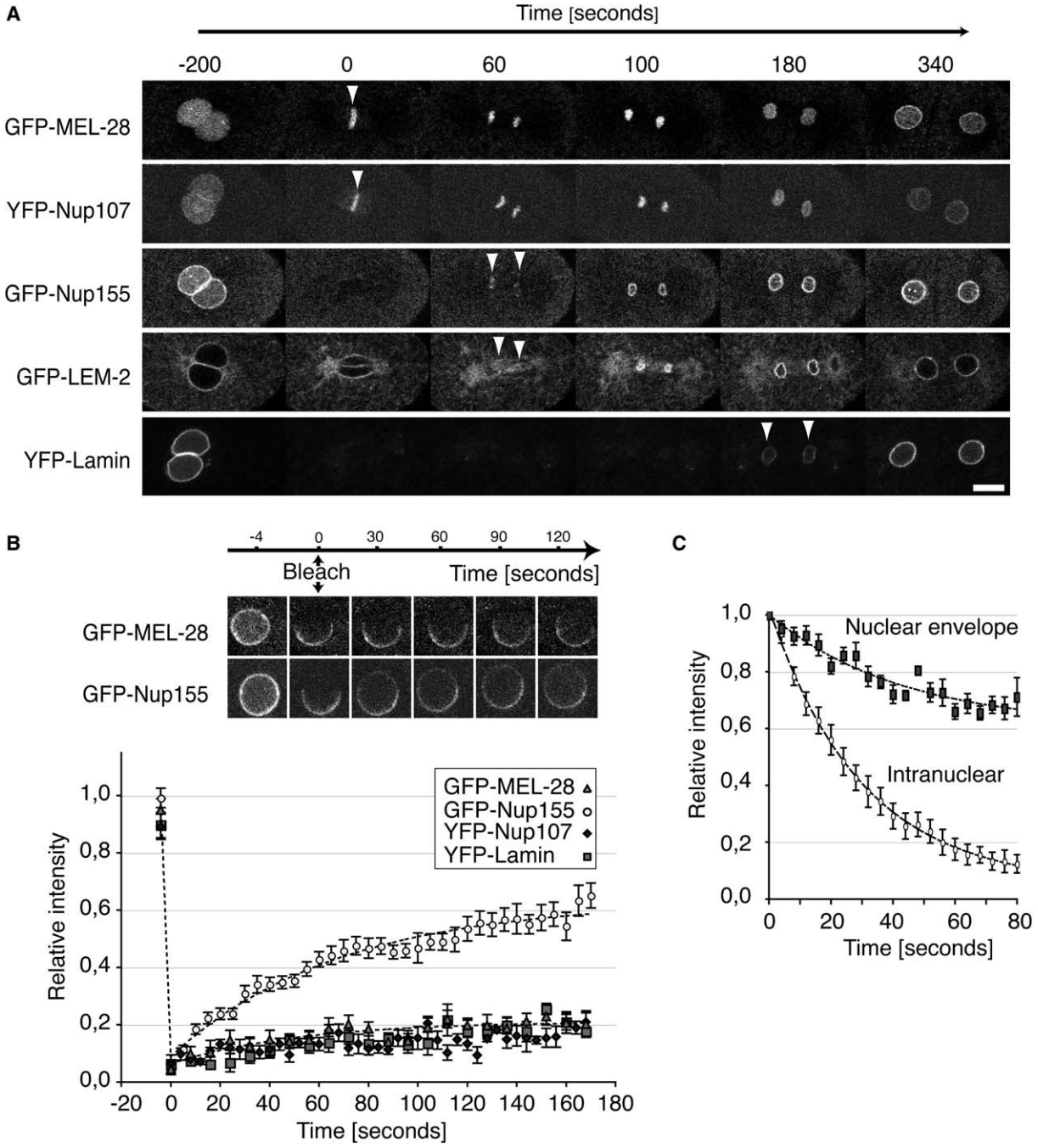

Figure 3. MEL-28 Is an Early-Recruited and Stable NE Protein

(A) Confocal still images from time-lapse recordings of NE proteins during the first mitotic division. All recordings were synchronized relative to anaphase onset. Arrowheads show the time of recruitment of Nup155, LEM-2, and Lamin, whereas MEL-28 and Nup107 were visible on chromatin throughout mitosis. The scale bar represents 10 μm.

(B) Confocal still images from FRAP experiments with nuclei of four-cell stage embryos expressing GFP-MEL-28 (top row) or GFP-Nup155 (bottom row). Fluorescence intensity was measured in six randomly chosen spots along the NE (three in the bleached region and three in the nonbleached region). Average values of the ratio of the intensity in bleached regions compared to the intensity in nonbleached regions for GFP-MEL-28 (triangles, n = 8), GFP-Nup155 (circles, n = 13), YFP-Lamin (squares, n = 4), and YFP-Nup107 (diamonds, n = 5) were measured in several nuclei.

(C) FLIP analysis of GFP-MEL-28. Fluorescent intensity was measured inside the nucleus and at the NE during continuous bleaching of approximately 30% of the nuclear volume (n = 6) and calculated relative to the intensity at time 0. All values were corrected for photobleaching occurring outside the main bleaching area.

MEL-28 and nucleoporins, including members of the early-assembling Nup107-160 complex, by coimmunoprecipitation were unsuccessful, possibly because of the very low solubility of MEL-28 in total worm protein extracts (data not shown). Ongoing yeast 2-hybrid analysis with *C. elegans* MEL-28 as bait has also so far failed

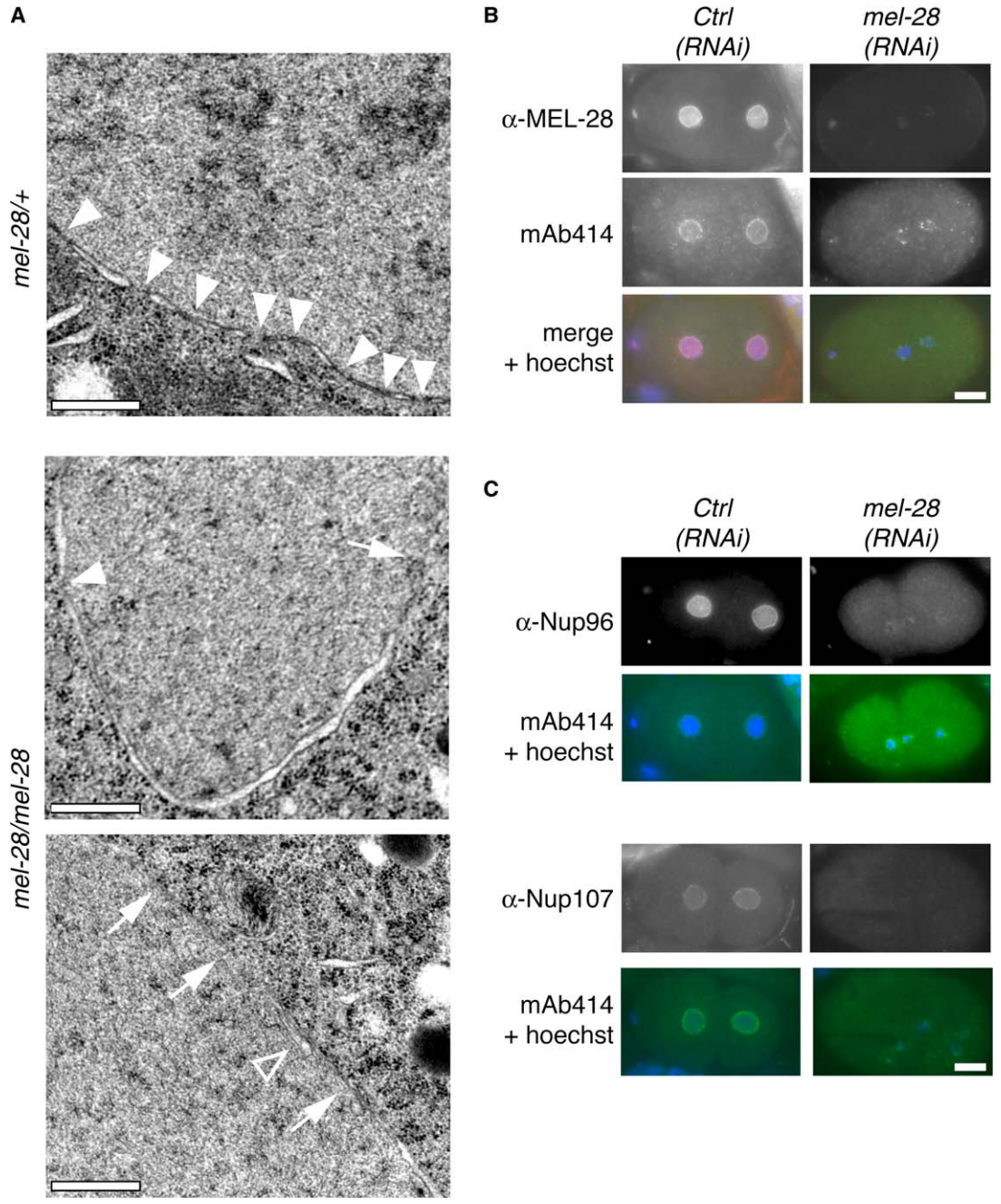

Figure 4. MEL-28 Depletion Affects Nuclear-Membrane Structure and NPC Assembly

(A) Gravid hermaphrodites were fixed by high-pressure freezing and sectioned so that embryos could be analyzed in utero by transmission electron microscopy (TEM). Embryos from heterozygous *mel-28(t1684)* hermaphrodites contained nuclei enclosed by continuous NEs with a high density of NPCs (top, white arrowheads), and embryos from homozygous *mel-28(t1684)* hermaphrodites showed defects in NE formation ranging from patchy association of chromatin with nuclear membranes in one- to four-cell embryos (bottom, the open arrowhead indicates apparently nonfused nuclear membranes, and arrows indicate chromatin not covered by membranes) to nuclei in older embryos with incomplete NEs containing only a few NPCs (middle, the white arrowhead points toward a single NPC and, the arrow indicates chromatin not covered by membranes). Scale bars represent 500 nm.

(B) Immunolocalization of MEL-28 (red in merge) and mAb414-reactive nucleoporins (green in merge) combined with Hoechst (blue in merge) staining of chromatin in two-cell embryos treated with control (left) or *mel-28* (right) dsRNA revealed an efficient depletion of MEL-28 and an abnormal nucleoporin distribution. The scale bar represents 10 μm.

(C) RNAi against MEL-28 (right) caused a strong decrease in Nup96 (top) and Nup107 (bottom) chromatin association as compared with that in control embryos (left). Merged images show localization of mAb414-reactive nucleoporins (green) and chromatin (blue). The scale bar represents 10 μm.

to identify MEL-28 interaction partners (J. Reboul, personal communication). This makes it difficult to assign a precise functional role to MEL-28 at this point, but it is hoped that further analysis of *C. elegans* MEL-28 and its homologs in other species will allow for a more detailed understanding of its function.

Experimental Procedures

Nematode Strains

Wild-type *C. elegans* Bristol strain N2, DP38 (*unc-119(ed3)*) [24], and GE2633 (*mel-28(t1684)*) [7] were obtained from the *Caenorhabditis* Genetic Center. Other strains used were XA3501 (*gfp::tbb-2; gfp::his-11*), XA3504 (*gfp::emr-1*) [18], XA3502 (*yfp::lmn-1*), XA3507 (*gfp::lem-2*) [8], XA3546 (*gfp::npp-8*), and XA3506 (*yfp::npp-5*) [16]. *mel-28(t1579)*, *mel-28(t1589)*, and *mel-28(t1578)* [7] were kindly provided by Ralph Schnabel. *mel-28(t1684)* was crossed with XA3502 and WH204 (*gfp::tbb-2*) [25] to obtain, respectively, XA3535 and XA3531. A strain expressing GFP-SP12 was kindly provided by Anne Spang and John White [11]. Strains XA3556 (*gfp::mel-28*), XA3537 (*mel-28::TAP*), XA3552 (*mel-28(t1579);mel-28::TAP*), and XA3545 (*gfp::him-10*) were generated in this study.

Plasmid Constructions and Transgenesis

A GFP-MEL-28 expression plasmid pPAG28 was constructed by replacing *his-11* downstream of *gfp* in pJH4.52 [25] with a genomic sequence encoding MEL-28. Transgenic worms were generated by transformation of DP38 with a 1:1 mixture of pPAG28 and pDP#MM051 vectors [24]. A *mel-28*-specific RNAi construct was cloned into pPD129.36 L4440 and transformed into *E. coli* strain HT115(DE3) [26]. In RNAi experiments, empty pPD129.36 vector was the negative control. For MEL-28 antibody production, amino acids 990–1237 of MEL-28 were expressed in *E. coli*, purified, and injected into rabbits (see Supplemental Experimental Procedures).

RNAi

For RNA interference, worms were fed with bacteria that express double-stranded RNA (dsRNA) [18]. For imaging, L4 larvae from GFP strains were incubated on RNAi plates at 20°C for 32-40 hr. For Western blots, approximately 3000 synchronized N2 L4 larvae were incubated for 35 hr at 20°C. Adult worms were collected and bleached to release RNAi-treated embryos. The embryos were washed three times in M9 buffer, lysed directly in boiling SDS PAGE loading buffer, and vortexed for 3 min together with 0.1–0.3 mm diameter glass beads.

Live Imaging

Embryos were analyzed by time-lapse fluorescent microscopy on a Perkin Elmer Spinning Disc Confocal Ultraspin RS and by dual DIC and fluorescent microscopy on a Leica confocal microscope TCS SP2 with HCX PL APO 63×/1.4 objective. Images were collected at 7–20 s intervals. Laser intensities were adjusted so as not to affect development.

Immunofluorescence

Embryos were fixed and prepared for staining [18] with the following antibodies diluted in PBS with 0.1% Tween-20: anti-MEL-28 rabbit polyclonal serum (BUD3) (1:500); monoclonal antibody (mAb) 414 against nucleoporins (Jackson Immunoresearch Laboratories, West Grove, PA, 1:400); Cy5-conjugated donkey anti-rat secondary antibody (Jackson Immunoresearch Laboratories, 1:500); and goat anti-mouse Alexa Fluor 488 and 546 (Molecular Probes, Eugene, OR, 1:1000). For DNA staining, Hoechst 33258 (Hoechst, Germany) was used at 1 μg/ml. Confocal images were obtained with a Leica TCS SP2. Wide-field fluorescent images were obtained on a Leica DMRXA coupled to a Hamamatsu ORCAII-ER CCD camera controlled by Openlab software (Improvision).

Transmission Electron Microscopy

mel-28(t1684) heterozygous or homozygous hermaphrodites were transferred to planchettes, cryoimmobilized immediately with a Leica EMPact high-pressure freezer (Leica, Vienna, Austria), and processed [16].

Sections for immunolabeling were incubated at room temperature on drops of 5% bovine serum albumin (BSA) in PBS for 20 min and then incubated for 2 hr with affinity-purified MEL28 antibody diluted 1:20 in PBS. After three 30 min washes with drops of 0.25% Tween-20 in PBS, sections were incubated for 1 hr with goat anti-rabbit IgG coupled to 10 nm diameter colloidal gold particles (British BioCell International, Cariff, UK) diluted 1:50 in PBS. This was followed by three washes with drops of PBS for 5 min, two washes with distilled water, and air-drying. Omitting the primary polyclonal antibody controlled for nonspecific labeling. Control samples did not show any labeling. Sections were stained with 2% uranyl acetate in methanol and lead citrate and observed in a JEM-1010 electron microscope (Jeol, Japan).

Supplemental Data

Supplemental Data include Experimental Procedures, six figures, one table, and two movies and can be found with this article online at http://www.current-biology.com/cgi/content/full/16/17/1748/DC1/.

Acknowledgments

P.A. is indebted to C. González for providing generous support. Some *C. elegans* strains used in this work were provided by the *Caenorhabditis* Genetic Center, funded by the National Institutes of Health National Center for Research Resources. We also thank R. Schnabel, A. Spang, and J. White for providing strains and A. Hyman for communicating unpublished data. P.A. was supported by the Deutsche Forschungsgemeinschaft and the Spanish Ministry of Education and Science (RYC-2003-001521, BFU2004-01096). V.G. was funded by the Fondation pour la Recherche Médicale. All authors except C.L.I. were supported by the European Molecular Biology Laboratory.

Received: March 28, 2006
Revised: May 16, 2006
Accepted: June 1, 2006
Published: September 5, 2006

References

1. Prunuske, A.J., and Ullman, K.S. (2006). The nuclear envelope: Form and reformation. Curr. Opin. Cell Biol. *18*, 108–116.
2. Hetzer, M., Walther, T.C., and Mattaj, I.W. (2005). Pushing the envelope: Structure, function, and dynamics of the nuclear periphery. Annu. Rev. Cell Dev. Biol. *21*, 347–380.
3. Antonin, W., Franz, C., Haselmann, U., Antony, C., and Mattaj, I.W. (2005). The integral membrane nucleoporin pom121 functionally links nuclear pore complex assembly and nuclear envelope formation. Mol. Cell *17*, 83–92.
4. Fraser, A.G., Kamath, R.S., Zipperlen, P., Martinez-Campos, M., Sohrmann, M., and Ahringer, J. (2000). Functional genomic analysis of C. elegans chromosome I by systematic RNA interference. Nature *408*, 325–330.
5. Gönczy, P., Echeverri, C., Oegema, K., Coulson, A., Jones, S.J., Copley, R.R., Duperon, J., Oegema, J., Brehm, M., Cassin, E., et al. (2000). Functional genomic analysis of cell division in C. elegans using RNAi of genes on chromosome III. Nature *408*, 331–336.
6. Sonnichsen, B., Koski, L.B., Walsh, A., Marschall, P., Neumann, B., Brehm, M., Alleaume, A.M., Artelt, J., Bettencourt, P., Cassin, E., et al. (2005). Full-genome RNAi profiling of early embryogenesis in Caenorhabditis elegans. Nature *434*, 462–469.
7. Gönczy, P., Schnabel, H., Kaletta, T., Amores, A.D., Hyman, T., and Schnabel, R. (1999). Dissection of cell division processes in the one cell stage Caenorhabditis elegans embryo by mutational analysis. J. Cell Biol. *144*, 927–946.
8. Galy, V., Mattaj, I.W., and Askjaer, P. (2003). Caenorhabditis elegans nucleoporins Nup93 and Nup205 determine the limit of nuclear pore complex size exclusion in vivo. Mol. Biol. Cell *14*, 5104–5115.
9. Brachner, A., Reipert, S., Foisner, R., and Gotzmann, J. (2005). LEM2 is a novel MAN1-related inner nuclear membrane protein associated with A-type lamins. J. Cell Sci. *118*, 5797–5810.
10. Lee, K.K., Gruenbaum, Y., Spann, P., Liu, J., and Wilson, K.L. (2000). C. elegans nuclear envelope proteins emerin, MAN1, lamin, and nucleoporins reveal unique timing of nuclear envelope breakdown during mitosis. Mol. Biol. Cell *11*, 3089–3099.
11. Poteryaev, D., Squirrell, J.M., Campbell, J.M., White, J.G., and Spang, A. (2005). Involvement of the actin cytoskeleton and homotypic membrane fusion in ER dynamics in Caenorhabditis elegans. Mol. Biol. Cell *16*, 2139–2153.

12. Oegema, K., Desai, A., Rybina, S., Kirkham, M., and Hyman, A.A. (2001). Functional analysis of kinetochore assembly in Caenorhabditis elegans. J. Cell Biol. *153*, 1209–1226.
13. Gunsalus, K.C., Ge, H., Schetter, A.J., Goldberg, D.S., Han, J.D., Hao, T., Berriz, G.F., Bertin, N., Huang, J., Chuang, L.S., et al. (2005). Predictive models of molecular machines involved in Caenorhabditis elegans early embryogenesis. Nature *436*, 861–865.
14. Howe, M., McDonald, K.L., Albertson, D.G., and Meyer, B.J. (2001). HIM-10 is required for kinetochore structure and function on Caenorhabditis elegans holocentric chromosomes. J. Cell Biol. *153*, 1227–1238.
15. Salina, D., Enarson, P., Rattner, J.B., and Burke, B. (2003). Nup358 integrates nuclear envelope breakdown with kinetochore assembly. J. Cell Biol. *162*, 991–1001.
16. Franz, C., Askjaer, P., Antonin, W., Iglesias, C.L., Haselmann, U., Schelder, M., de Marco, A., Wilm, M., Antony, C., and Mattaj, I.W. (2005). Nup155 regulates nuclear envelope and nuclear pore complex formation in nematodes and vertebrates. EMBO J. *24*, 3519–3531.
17. Belgareh, N., Rabut, G., Bai, S.W., van Overbeek, M., Beaudouin, J., Daigle, N., Zatsepina, O.V., Pasteau, F., Labas, V., Fromont-Racine, M., et al. (2001). An evolutionarily conserved NPC subcomplex, which redistributes in part to kinetochores in mammalian cells. J. Cell Biol. *154*, 1147–1160.
18. Askjaer, P., Galy, V., Hannak, E., and Mattaj, I.W. (2002). Ran GTPase cycle and importins alpha and beta are essential for spindle formation and nuclear envelope assembly in living Caenorhabditis elegans embryos. Mol. Biol. Cell *13*, 4355–4370.
19. Walther, T.C., Alves, A., Pickersgill, H., Loiodice, I., Hetzer, M., Galy, V., Hulsmann, B.B., Kocher, T., Wilm, M., Allen, T., et al. (2003). The conserved Nup107–160 complex is critical for nuclear pore complex assembly. Cell *113*, 195–206.
20. Daigle, N., Beaudouin, J., Hartnell, L., Imreh, G., Hallberg, E., Lippincott-Schwartz, J., and Ellenberg, J. (2001). Nuclear pore complexes form immobile networks and have a very low turnover in live mammalian cells. J. Cell Biol. *154*, 71–84.
21. Rabut, G., Doye, V., and Ellenberg, J. (2004). Mapping the dynamic organization of the nuclear pore complex inside single living cells. Nat. Cell Biol. *6*, 1114–1121.
22. Harel, A., Orjalo, A.V., Vincent, T., Lachish-Zalait, A., Vasu, S., Shah, S., Zimmerman, E., Elbaum, M., and Forbes, D.J. (2003). Removal of a single pore subcomplex results in vertebrate nuclei devoid of nuclear pores. Mol. Cell *11*, 853–864.
23. Cronshaw, J.M., Krutchinsky, A.N., Zhang, W., Chait, B.T., and Matunis, M.J. (2002). Proteomic analysis of the mammalian nuclear pore complex. J. Cell Biol. *158*, 915–927.
24. Maduro, M., and Pilgrim, D. (1995). Identification and cloning of unc-119, a gene expressed in the Caenorhabditis elegans nervous system. Genetics *141*, 977–988.
25. Strome, S., Powers, J., Dunn, M., Reese, K., Malone, C.J., White, J., Seydoux, G., and Saxton, W. (2001). Spindle dynamics and the role of gamma-tubulin in early Caenorhabditis elegans embryos. Mol. Biol. Cell *12*, 1751–1764.
26. Timmons, L., and Fire, A. (1998). Specific interference by ingested dsRNA. Nature *395*, 854.